Optical Materials: X 12 (2021) 100101

Contents lists available at ScienceDirect

Optical Materials: X

journal homepage: www.journals.elsevier.com/optical-materials-x

Invited Article

(INVITED) Design of symmetric nanoresonators to scale the ultrafast optical modulation in plasmonic metasurfaces

Andrea Schirato [a,b], Margherita Maiuri [a,c,*]

[a] Dipartimento di Fisica, Politecnico di Milano, Piazza Leonardo da Vinci 32, 20133, Milan, Italy
[b] Istituto Italiano di Tecnologia, Via Morego 30, 16163, Genoa, Italy
[c] Istituto di Fotonica e Nanotecnologie – Consiglio Nazionale Delle Ricerche, Piazza Leonardo da Vinci 32, 20133, Milan, Italy

ARTICLE INFO

Keywords:
Ultrafast nanophotonics
Plasmonic metasurfaces
Symmetry breaking
Pump-probe spectroscopy

ABSTRACT

The light-driven control over the properties of optical nanostructured materials has been shown to be a promising route to achieve various functionalities, possibly on sub-picosecond time scales when ultrashort pulses are employed. Here, we discuss how to induce and reveal an ultrafast dichroism in a set of plasmonic metasurfaces with increasing symmetry by using femtosecond pump-probe spectroscopy. We show that such effect is general, promoted by the photogeneration of out-of-equilibrium electrons, and it can be induced in any sufficiently large nanoresonator, provided that plasmonic modes with well-defined symmetry are excited. The intensity of the photoinduced ultrafast dichroisms depends on the geometry of the nanoresonator, and scales up when the excitation symmetry of the plasmonic mode decreases. Our comparative analysis demonstrates the possibility to exploit light-matter interaction as an effective tool to manipulate transient optical symmetry of metasurfaces.

1. Introduction

Recent technological advancements in the design of optical nanostructured materials [1,2], especially in two-dimensional configuration, namely as metasurfaces [3,4], have boosted intensive research aiming at regulating their properties [5,6] to achieve diverse functionalities [7–9]. The light-driven control of an optical metasurface has been even obtained on a sub-picosecond time scale by employing ultrashort pulse illumination [10,11], opening the way to the sparkling research field of ultrafast nanophotonics [12]. This is especially true for metasurfaces based on plasmonic materials [13,14], by virtue of the very efficient nonlinear processes promoting the generation of energetic (hot) electrons [15–17]. Among different kinds of all-optical manipulation techniques, ultrafast polarization switching has attracted a huge interest for advanced applications in photonics and beyond, based on a variety of materials, from metals and semiconductors to 2D materials [18–23].

In this framework, experimental approaches based on a polarization-resolved pump-probe spectroscopy scheme exploiting nonlinear light-matter interaction have been lately employed to reveal and control a photoinduced anisotropy signal in an otherwise isotropic plasmonic metasurface, thus promoting pump-induced dichroism [24,25]. It has been shown [24] that the intense ultrashort light pulse induces spatio-temporal transients which can break the symmetry of the gold nanostructure composed of high symmetric meta-atoms in the shape of nanocrosses (NCs). The generated dichroic modulation is broadband and returns to the isotropic state within a few hundreds of fs, i.e. well before the complete relaxation of the nanostructure (which rather requires tens of ps [26–28]). Thus, the main contribution to this phenomenon arises from non-thermal carriers, while thermalized carriers, which undergo a diffusion process at the nanoscale, contribute less [21,29].

This remarkable result raises questions on the general validity of such an effect, considering the given symmetry of the NC metasurface studied. Here we address such question by employing numerical modelling to design a set of periodically arranged metal nanoresonators with increasing symmetry, calculate their ultrafast photoinduced dichroic response and compare them with the transient anisotropic pump-probe signal measured on the NC metasurface. Interestingly, we found that such behavior is universal, since it is promoted by the photogeneration of out-of-equilibrium electrons of the meta-atoms, a general property of metallic nanostructures (governed by their third-order thermo-modulational nonlinearities [30,31]), and could even be extended to other systems with strong nonlinearities such as semiconductors or graphene. Indeed, we predict a dichroic response can be induced in any nanoresonator, provided that plasmonic modes with

* Corresponding author. Dipartimento di Fisica, Politecnico di Milano, Piazza Leonardo da Vinci 32, 20133, Milan, Italy.
E-mail address: margherita.maiuri@polimi.it (M. Maiuri).

https://doi.org/10.1016/j.omx.2021.100101
Received 31 August 2021; Received in revised form 20 September 2021; Accepted 2 October 2021
Available online 9 October 2021

well-defined symmetry and featuring significant spatial inhomogeneities across the single meta-atom are resonantly excited. This condition is more efficiently fulfilled in sufficiently large structures, with size comparable to the wavelength of the electromagnetic field. The calculated transient dichroism scales with the degree of symmetry of the structure geometry chosen: it is weaker in a metasurface made of gold nanodisks (NDs) and stronger if gold nanoplates (NPs) are considered. Furthermore, NPs and NCs metasurfaces share the same geometrical symmetry, however the calculated transient dichroism (close to the signal peak, across the spectral range of interest) in the NCs is ~2.5 times larger than the one found in the NPs nanostructure. We rationalize this effect by observing that for a given polarization state of the exciting light, plasmonic modes in NPs and NCs exhibit substantially different spatial confinement across the meta-atom. This produces a stronger (weaker) dichroism for the more (less) spatially-confined mode, in NCs (NPs) meta-atoms.

Our study highlights the role of design of single nanostructures, here focussed to explore symmetry as a degree of freedom, in controlling both the optical response of metasurfaces and the modulation of their properties upon ultrashort laser pulse illumination.

2. Methods

2.1. Ultrafast pump probe spectroscopy

The pump–probe set-up employed for the ultrafast experiments is briefly described here. An amplified Ti:sapphire laser produces 100-fs pulses, centered at 800 nm, operating at 2-kHz repetition rate, which are used to pump two non-collinear optical parametric amplifiers to generate the pump and probe pulses, respectively. The pump pulses cover the 850–950-nm bandwidth and were compressed by a fused-silica prism pair to sub-30-fs duration, while the probe pulses cover the 565–735-nm bandwidth and were compressed by chirped mirrors to sub-10-fs duration. Further details on the experimental apparatus can be found elsewhere [32].

The pump and probe were focused by a spherical mirror to a diameter of 50 μm, smaller than the sample area patterned with NCs. The pump fluence was kept at 400 $\mu J/cm^2$. The NCs metasurface was aligned perpendicular to the probe beam. The transmitted probe was dispersed in a spectrometer and detected with a custom-made charge-coupled device operating at the full laser repetition rate. To perform polarization-resolved pump probe experiments, we kept the pump polarization parallel to one of the arms of the crosses, while the probe polarization was fixed at an angle of 45° with respect to the pump, and then we performed polarization filtering of the parallel and perpendicular components of the transmitted probe pulse right before the detection. The pump pulse was modulated at 1 kHz by a mechanical chopper and the relative differential transmittance signal in parallel ($\Delta T/T_{\parallel}$) and perpendicular ($\Delta T/T_{\perp}$) configuration was measured as a function of probe wavelength λ and pump–probe delay τ.

2.2. Numerical modelling

To predict the ultrafast optical response of plasmonic nanostructures upon laser pulse illumination and reproduce pump-probe measurements, we employed a numerical semi-classical approach, describing the sub-ps energy relaxation processes at the nanoscale following photoabsorption [33,34]. The model, reported in Ref. [24] and referred to as the Inhomogeneous Three-Temperature Model (I3TM), is based on the well-established 3TM [35,36]. In particular, it extends the latter most common formulation by accounting for a space dependence of the internal degrees of freedom detailing hot carrier dynamics in photoexcited metallic nanosystems [37–39]. These are the excess energy density stored in a non-thermal portion of the electronic population, N, a temperature associated to thermalized electrons, Θ_E, and the Au phonon temperature Θ_L, interlinked by a set of partial differential rate equations, reading:

$$\frac{\partial N}{\partial t} = -aN - bN + P_{\text{abs}}(\boldsymbol{r}, t) \tag{1}$$

$$C_E\frac{\partial \Theta_E}{\partial t} = -\nabla(-\kappa_E \nabla\Theta_E) - G(\Theta_E - \Theta_L) + aN \tag{2}$$

$$C_L\frac{\partial \Theta_L}{\partial t} = \kappa_L \nabla^2\Theta_L + G(\Theta_E - \Theta_L) + bN \tag{3}$$

The coefficients in the rate equations above, derived from comparison with first principle calculations (see e.g. Refs. [40–44] and references therein), either describe the electrons and phonons thermal properties (heat capacities C_E, C_L and thermal conductivities κ_E, κ_L) or they account for electron-electron and electron-phonon scattering events undergone by the photoexcited both nonthermal (coefficients a, b) and thermalized (G) portion of the electronic population. The term driving the evolution of the three quantities is represented by the instantaneous absorbed power density, $P_{\text{abs}}(\boldsymbol{r}, t)$, which, in the I3TM, includes the exact spatial pattern of pump pulse absorption across the nanostructure (exceeding the limits of the Quasi Static Theory) via full-wave electromagnetic simulations. Furthermore, to simulate the dynamics of the differential transmittance, a model of Au thermo-modulational nonlinearities has been employed to derive the space-time evolution of metal permittivity, starting from the one of the aforementioned energetic degrees of freedom [30,45]. Further details on the approach pursued can be found in Ref. [24]. The semiclassical description of hot carrier photogeneration and ultrafast relaxation and corresponding Au permittivity modulation is integrated in a Finite Element Method-based comprehensive simulation, modelling light-matter interaction at the nanoscale. Periodic boundary conditions for the electromagnetic field are imposed to model a perfectly periodic and infinite array of nanoresonators.

2.3. Sample fabrication

The metasurface experimentally investigated consists of a 2D squared arrangement of closely packed cross-shaped meta-atoms, fabricated by electron beam lithography on a CaF_2 substrate. The obtained meta-atoms have thickness 45 nm, width 60 nm and length 165 nm, with periodicity ~270 nm. Details on the fabrication procedure can be found elsewhere [24].

3. Results and discussions

3.1. Ultrafast experiments on gold nanocross metasurface

The fingerprint of an ultrafast photoinduced anisotropy can be revealed by exploiting a polarization-resolved pump-probe experiment. For the case of a metasurface made of isotropic gold nanocrosses, a broadband transient dichroism vanishing within less than 1 ps, when the initial isotropic state is recovered, was observed and discussed in great detail in a recent work [24]. Briefly, in such an experiment, the resonant excitation by a pump pulse with linear polarization along the direction of one of the arms of the nanocross creates an asymmetric absorption pattern in each meta-atom, locally affecting the electronic population of the metal. This in turn induces a non-uniform out-of-equilibrium hot carrier distribution, which anisotropically modifies the metal permittivity in the early times following photoexcitation. Upon resonant pump excitation, the plasmonic mode is mostly localized along that direction, keeping memory of the longitudinal resonance of the arms. Indeed, the cross shape represents a simple choice of a structure with high-symmetry geometry as well as strongly confined resonant near fields, offering a route to effectively discriminate the orientation of the excited plasmon mode.

The pump-induced transient anisotropy is detected by interrogating

the metasurface with probe pulses projected onto two co-orthogonal polarization directions defined with respect to the pump polarization orientation, leading to a differential transmittance signal in parallel ($\Delta T/T_{\parallel}$) or perpendicular ($\Delta T/T_{\perp}$) configuration. The results of the pump-probe experiments are reported in Fig. 1a (for probe polarization parallel to the pump one) and 1b (when pump and probe polarization are orthogonal). The two $\Delta T/T$ signals should be identical in the case of structures which are symmetric with respect to the directions analyzed. However, by inspecting the measured pump-probe maps over a broad range of wavelengths, a difference in the intensity between the two is recorded. Both spectral and temporal features differ between $\Delta T/T_{\parallel}$ (Fig. 1a) and $\Delta T/T_{\perp}$ (Fig. 1b). The latter displays a lower intensity (in absolute value) in the broad negative band, from 560 nm to ~720 nm. A peak between 640 nm and 680 nm is reached in a few hundreds of fs, following the typical dynamics of pump-probe differential transmittance traces from plasmonic structures [46–48]. The onset of a further band can be observed at higher energies for the $\Delta T/T_{\perp}$ signal (Fig. 1b), with a decrease of the signal intensity between 570 nm and 600 nm, both these features being less pronounced in the parallel map (Fig. 1a). Differences between maps observed during the first hundreds of fs following excitation vanish for pump-probe time delays longer than ~1 ps (corresponding to the recovery of the isotropic case, prior to the return to equilibrium which requires tens of ps, out of the experimental temporal scale measured).

The effect observed in pump-probe measurements is theoretically explained in terms of the spatio-temporal dynamics of the hot carrier population, generated by pump absorption within the single NC. The hot carrier population evolution both in time and space governs the anisotropic permittivity modulation across the meta-atom. Calculated pump-probe maps of the differential transmittance are shown in Fig. 1c and d, based on the numerical model followed in Ref. [24].

Simulated signals are in good agreement with the measurements, supporting the experimental observation of a transient dichroism. The main spectral and dynamical features of the signals are retrieved for the two polarizations, by describing transient changes in the optical properties of the metasurface, accounting for the internal relaxation processes of (both non thermal and thermalized) electrons.

To quantify and visualize the discrepancies between the two polarization-selective pump-probe maps, the signal difference $\Delta T/T_{\perp} - \Delta T/T_{\parallel}$ is defined. This quantity is broadband, evolves in time and it directly correlates with the photoinduced anisotropy across the meta-atoms.

In particular, spectra of the measured $\Delta T/T_{\perp} - \Delta T/T_{\parallel}$ evaluated at different pump-probe delays are reported in Fig. 2a over a broad spectral range (data are truncated above 730 nm due to lower signal-to-noise ratio limited by higher probe pulse dispersion). A dichroic signal reaching some percent at short time delays is observed, which is remarkable considering this is the same order of magnitude as the pump-probe traces. Simulations (Fig. 2b), except for a slight quantitative mismatch in intensity [24], well reproduce the experiments, in the spectral feature of the positive band of the dichroism as well as in the temporal dynamics of the signal. Both measured and computed dichroism significantly decrease from 150 fs (blue traces in Fig. 2) to 850 fs (light blue), approaching zero for longer pump-probe delays. The time evolution of the signal is shown for an exemplary probe wavelength selected at ~580 nm, both in the experiment (Fig. 2c) and in the simulation (Fig. 2d) displaying the decay of the transient signal and its ultrafast recovery within 1 ps.

3.2. Higher symmetry nanoresonator design

To demonstrate that the transient photoinduced dichroism observed in the NC metasurface is a general phenomenon occurring in plasmonic nanostructures, numerical simulations have been performed on metallic nanoresonators (in planar periodic arrangement) featuring different geometrical symmetries.

In quasi-2D configuration, the most symmetric structure to analyze is a disk-shaped one, having a C_{∞} symmetry around its axis, in the (zy) plane. When illuminated with a plane wave at normal incidence and linear polarization (Fig. 3a), its optical response is perfectly isotropic for any direction of the incoming electric field. Thus, the corresponding metasurface, obtained as the ordered arrangement of identical NDs in a square lattice, inherits from its unit cell the same symmetry properties. Specifically, to better compare the optical performances among different

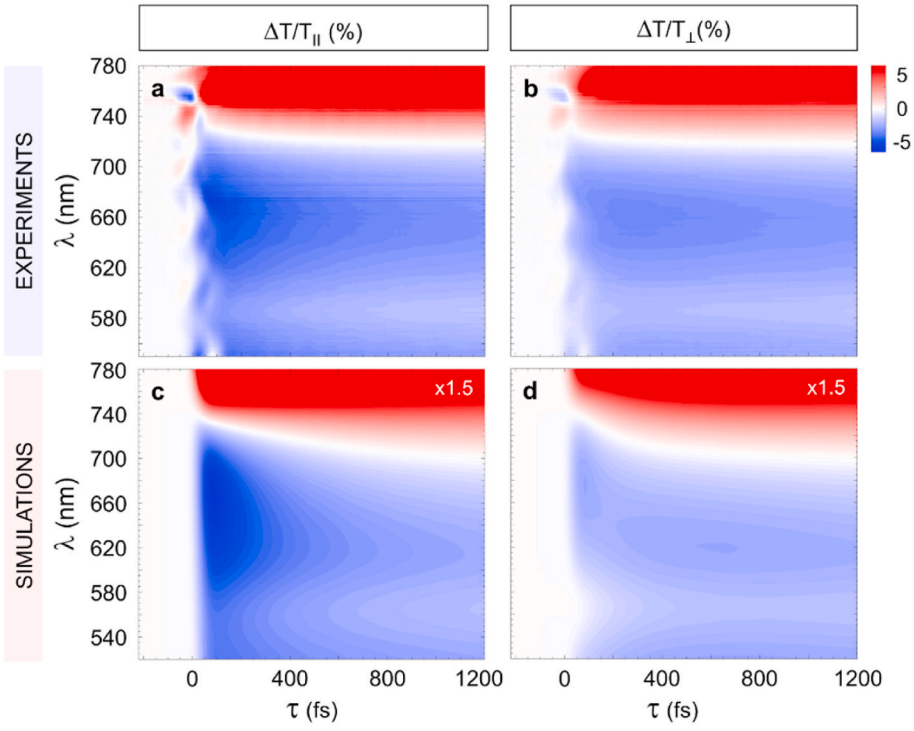

Fig. 1. Transient anisotropy revealed by polarization-resolved pump-probe spectroscopy. Experimental (a, b) and simulated (c, d) maps of the differential transmittance, $\Delta T/T(\lambda, \tau)$, recorded in a broadband polarization-resolved ultrafast pump-probe spectroscopy scheme. The pump pulse is linearly polarized along the direction of one of the cross-shaped meta-atom arms. Probe pulses, impinging on the sample with a time delay τ are linearly polarized at 45° to the pump polarization. The transient signal is then analyzed along two co-orthogonal directions, either parallel ($\Delta T/T_{\parallel}$, panels a, c) or perpendicular ($\Delta T/T_{\perp}$, panels b, d) to the pump pulse polarization.

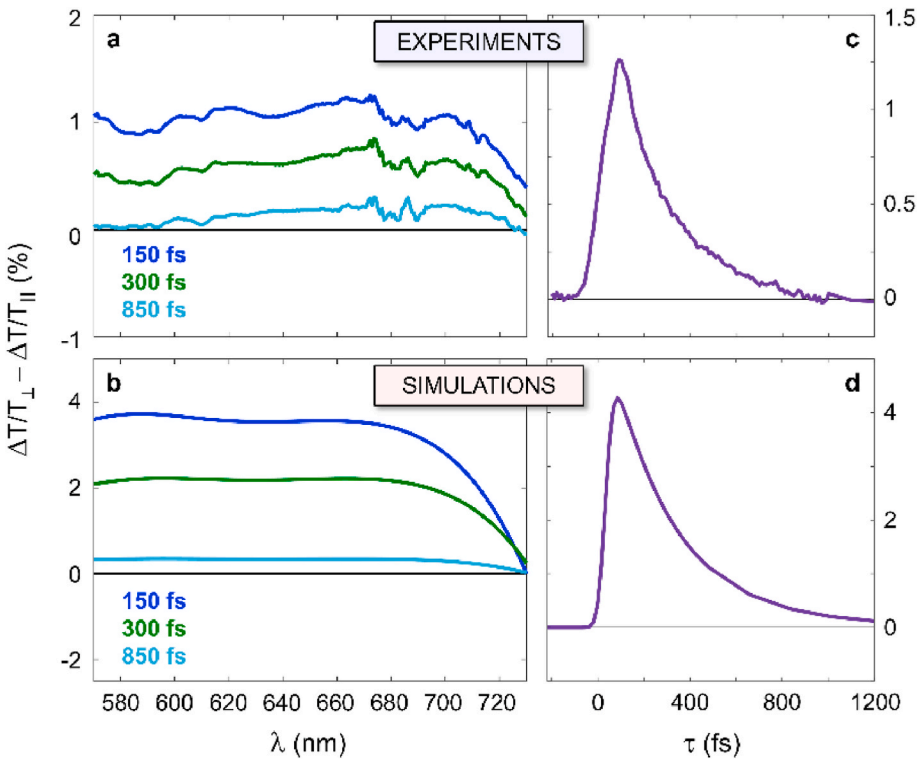

Fig. 2. Ultrafast dichroic spectra and dynamics. (a–b) Experimental (a) and simulated (b) spectra of the broadband dichroism, $\Delta T/T_{\perp} - \Delta T/T_{\parallel}$, photoinduced by pump pulse absorption, shown at some exemplary pump-probe time delays of 150 fs (blue), 300 fs (green), 850 fs (light blue). The difference in transient transmittance for the two polarizations vanishes on a sub-ps time range, demonstrating that the isotropic state of the metasurface is recovered within less than 1 ps. (c–d) Experimental (c) and simulated (d) time evolution of the transient dichroism evaluated at a probe wavelength of around 580 nm. (For interpretation of the references to colour in this figure legend, the reader is referred to the Web version of this article.)

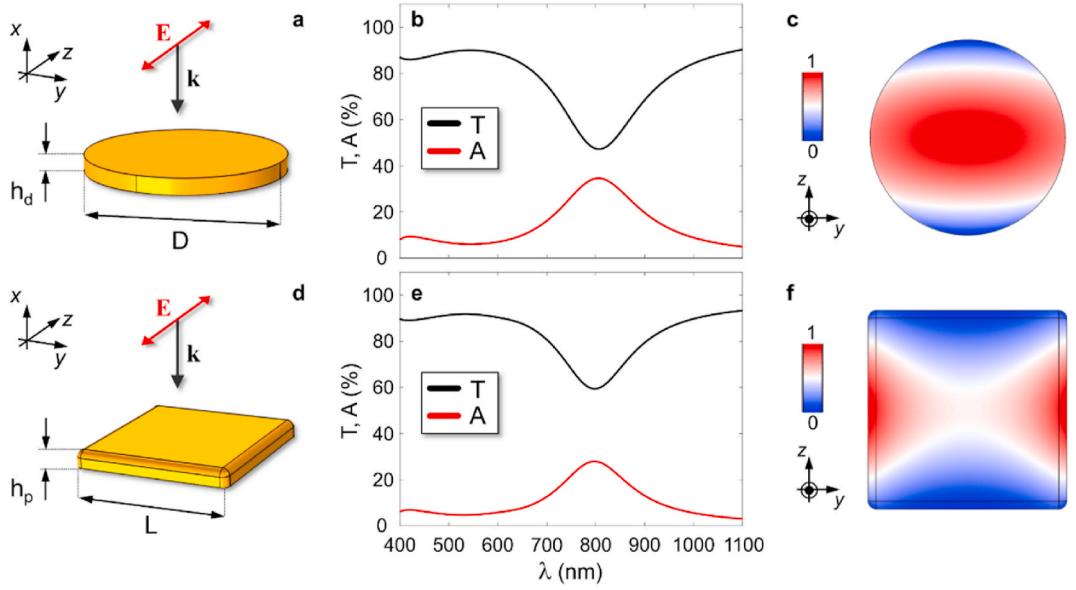

Fig. 3. Optical symmetry breaking in resonant structures. (a) Sketch of the resonant meta-atom geometry investigated, consisting of a gold nanodisk of diameter D = 125 nm, height h_d = 10 nm. (b) Optical response of the metasurface in static conditions, displayed in terms of transmission (black) and absorption (red). (c) 2D map (cross-sectional cut at x = h_d/2) of the normalized electromagnetic absorption across the meta-atom upon illumination at 860 nm. (d–f) Same as (a–c) for a squared plate of side L = 95 nm and height h_p = 10 nm. (For interpretation of the references to colour in this figure legend, the reader is referred to the Web version of this article.)

structures, the ND metasurface was designed to exhibit a static response comparable to the one measured for NCs [24]. Such correspondence is achieved by considering the NC array periodicity (285 nm in the simulations) as the center-to-center distance between neighbouring disk meta-atoms with diameter D = 125 nm and height h_d = 10 nm, lying on the same substrate (CaF_2) as the NC sample. The simulated response of the periodic structure is shown in Fig. 3b, featuring a clear resonant plasmonic behavior, i.e. a well-defined peak in absorption at ~800 nm, with spectral width close to the static spectra of NCs. Importantly, owing to the relatively large dimensions of the ND, the near fields are characterized by spatially-structured patterns across the particle, especially when resonant modes are excited, despite the high symmetry of the structure [38]. Thus, by considering an incoming plane wave linearly polarized along the *z* direction at a wavelength of 860 nm, namely on the red edge of the plasmon, the computed absorption spatial pattern, shown in Fig. 3c, exhibits a non-uniform profile within the single

resonator. For the geometrical parameters set, radiation is mostly absorbed in the center of the disk, and to a lesser degree on the edges in the z direction. This results in a symmetry breaking, induced by optical means, across the meta-atom. Its optical properties undergo a decrease in the degree of symmetry as a result of light absorption, which creates preferential optical axes in the structure. The ND is thus no longer invariant upon rotation by an arbitrary angle, with its perfect isotropy being broken.

NDs represent meta-atoms with the highest symmetry to be considered for our comparative purposes. As a further example of a symmetric nanoresonator, we considered a squared nanoplate (Fig. 3d). With the same rationale as for NDs, geometrical parameters of the corresponding NP metasurface were set to have static properties similar to NCs. To do so, plates with side L = 95 nm and height h_p = 10 nm were modelled. The unperturbed optical response of the resulting periodic structure is reported in Fig. 3e. As for the two structures already introduced, a typical plasmonic resonance is obtained, with spectral features close to the previous ones. By its C_4 symmetry, the NP metamaterial is isotropic with respect to excitations. As it will be shown later on in more detail, NPs are of particular interest, as their geometrical (and optical, once perturbed) symmetry is the same as NCs. Similarly to NDs, the plasmonic mode induced across the metallic meta-atom reveals spatial patterns with a lower optical symmetry, as shown in Fig. 3f, which reports the normalized electromagnetic absorbed power when a linearly polarized (aligned to the z-axis) plane wave at 860 nm illuminates the periodic structure. Also for NPs, photoabsorption is thus demonstrated to induce a symmetry breaking in the properties of the meta-atom inherited by the metasurface.

Similarly to the NC metasurface experimentally interrogated, light-driven anisotropy is promoted by out-of-equilibrium electrons, photogenerated in the metal with an inhomogeneous pattern governed by instantaneous absorption of radiation, i.e. the one in Fig. 3c for NDs, Fig. 3f for NPs. This is crucial for the intensity of the transient dichroic signal, which has been shown to be dominated by spatio-temporal non-thermal effects [24]. Once generated by the pump pulse, hot electrons undergo ultrafast relaxation and diffusion processes across the meta-atom. While relaxation rates are independent of the specific structure, diffusion is directly influenced by the spatial distribution of hot electrons. In these terms, the intensity of the transient dichroism is intimately related to the magnitude of the optical symmetry-breaking in the single nanoresonator.

By thus performing nonlinear dynamical simulations (see Methods Section), a transient dichroism is indeed predicted in the two structures. Fig. 4 shows the broadband dichroic signal, as previously defined for the NCs. Fig. 4a refers to the ND metasurface, while in Fig. 4b the same quantity is shown for NP meta-atoms. The transient dichroism, featuring a positive band between 500 nm and 720 nm and a negative one at longer wavelengths for the two metasurfaces, is weaker in the disk metasurface (Fig. 4a), as a consequence of the higher symmetry of the single meta-atom. Indeed, a more inhomogeneous distribution of photoexcited hot carriers promotes more intense permittivity modulation in the metal, thus introducing a larger difference in the optical properties probed by co-orthogonal polarizations (Fig. 4b).

3.3. Comparative analysis of the nanoresonators

The ultrafast dichroism obtained for the set of plasmonic metasurfaces with increasing symmetry can be directly compared to assess the impact of (geometrical, optical and modal) symmetry on the intensity of the transient anisotropic signal. Fig. 5 illustrates such comparison by displaying spectra of the transient dichroism for the three structures, starting from the one with highest symmetry (NDs, Fig. 5a) and decreasing, to NPs (Fig. 5b) and NCs (Fig. 5c and d) respectively. Broadband spectra are here reported for a pump-probe time delay of 200 fs, close to the dichroic signal peak, when the hot carrier distribution is still inhomogeneous across the meta-atom. The fact that the three

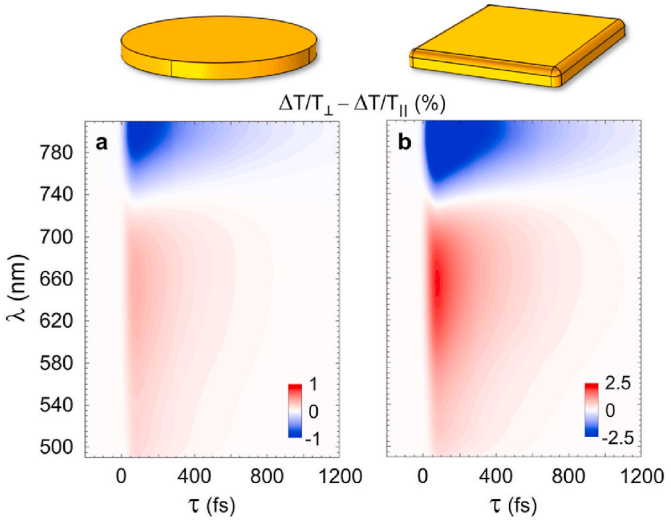

Fig. 4. Photoinduced dichroism in symmetric plasmonic structures. (a) Map of the simulated broadband dichroism, $\Delta T/T_{\perp} - \Delta T/T_{\parallel}$, photoinduced by pump pulse absorption (wavelength λ_p = 860 nm, fluence F_p = 300 μJ/cm^2, linear polarization along the z-direction) in a metasurface made of Au disks (top panel inset). (b) Same as (a) for nanoplate meta-atoms.

structures exhibit a sizeable non-zero ultrafast dichroic signal confirms the general nature of the effect of light-induced anisotropy, driven by hot carriers and supported by plasmon excitation.

Results also show that the intensity of dichroism scales with the degree of symmetry of the meta-atom. In the case of NDs, featuring the highest geometry, the pump-induced signal is the weakest. Then, by decreasing the degree of symmetry, the dichroism intensity is enhanced, moving to NPs and NCs. The signal is maximum for the latter and confirmed by experimental measurements (except for a ~2 factor in amplitude [24]). To quantitatively compare the structure performances, the simulated signal averaged over the spectral range analyzed for the fixed 200-fs delay is computed. In these terms, transient dichroism in NCs is proven to be ~2.5 times larger than in NPs, and ~13 times with respect to NDs, namely to scale with the degree of symmetry of the structure. To rationalize the observed difference in intensity, symmetry arguments can be invoked. In particular, the higher dichroism in NPs and NCs if compared to NDs could be explained by considering the higher geometrical symmetry of disk-shaped resonators (C_∞), which keep an overall more uniform pattern of absorption, correlating to the anisotropic permittivity modulation. However, a comparison between NPs and NCs suggests that geometrical symmetry should not suffice to explain the difference in signal intensity, since the two meta-atoms share the same C_4 symmetry. Moreover, for the pump polarization considered, the degree of symmetry of the light absorption pattern, which correlates with the hot carrier distribution, is also the same (as discussed in Ref. [24]). However, the plasmonic mode excited in NCs is much more spatially confined within the particle if compared to NPs (Fig. 3f and ref. 24). Its structure in space, reminiscent of the longitudinal plasmonic resonance of the single arm of the cross, entails a hot-carrier-driven dynamical modulation of permittivity which is much more inhomogeneous [24]. Modal confinement, more significant for NCs owing to its shape, is therefore expected to be the key aspect to interpret the weaker dichroism achieved in NP metasurface.

4. Conclusion

In this study, we have examined the photoinduced transient dichroism generated in a set of plasmonic metasurfaces with various degrees of symmetry. A polarization-resolved pump-probe spectroscopy scheme was employed to observe an ultrafast broadband anisotropy,

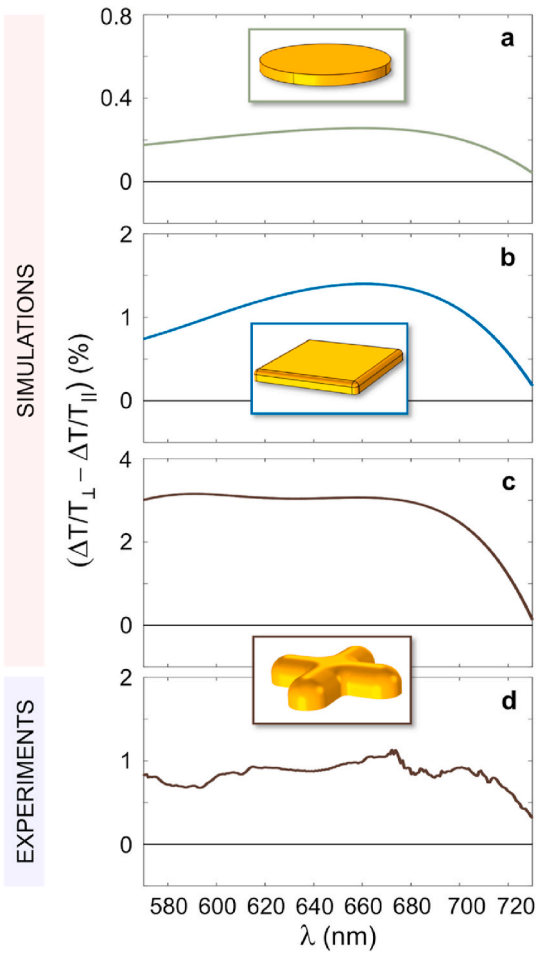

Fig. 5. Dichroism spectra for increasing symmetry. (a–c) Transient spectral cut of the simulated dichroic signal for the plasmonic metasurface consisting of nanodisks (a), nanoplates (b), nanocrosses (c) respectively, evaluated at a pump-probe delay of 200 fs. (d) Experimental dichroic signal for the gold nanocross metasurface sample, at the same time delay. (For interpretation of the references to colour in this figure legend, the reader is referred to the Web version of this article.)

which is related to the optical symmetry-breaking following pump absorption and governed by the spatio-temporal dynamics of photoexcited hot carriers. Experimental evidence, supported by a quantitative numerical model, of such an effect was recently reported [24] for a metasurface made of gold cross-shaped nanostructures. Since the broadband dichroism is driven by ultrafast relaxation and diffusion processes of out-of-equilibrium electrons, the return to isotropic optical properties occurs within less than 1 ps. However, this phenomenon per se has general validity and it does apply to any nanostructure upon suitable excitation conditions. To demonstrate it, we designed a set of metasurfaces made of plasmonic resonators with increasing symmetry, starting from the one with highest symmetry in quasi-2D configuration, i.e. a disk, to squared nanoplates. Relatively large structures were explored, able to support plasmonic modes with spatially structured patterns and well-defined symmetry profiles when excited by ultrashort pulses with a given polarization condition. This entails that hot carriers are photoexcited with an inhomogeneous distribution, which in turn dynamically governs the meta-atom transient anisotropy. The comparison of the computed and measured ultrafast dichroic signals for metasurfaces made of plasmonic resonators with increasing symmetry had a twofold interest. On the one hand, it numerically proved that the photoinduced dichroic response observed for NCs can be induced in structures with even higher symmetry, since it relates to the intrinsic capability of light excitation to anisotropically modulate the metal permittivity. Furthermore, our analysis also demonstrated that meta-atom symmetry can be designed to scale the intensity of the optical modulation effect. NDs, with the highest geometrical symmetry, are indeed shown to exhibit a weaker dichroism when compared to NPs and NCs. However, the geometry of the resonator itself is not the only aspect to be considered. The modal symmetry of the plasmonic resonance excited by the pump also has an impact on the transient dichroic signal, here predicted to be weaker in NPs than in NCs, since the latter feature a highly confined mode supporting hot carrier generation. Our results corroborate the relevance of designing nanoresonators and metasurfaces to implement and optimize optical functionalities, such as ultrafast polarization control. The exploitation of nanostructure symmetry to scale its ultrafast response also points in favour of the interest of engineering light-matter interaction for efficient all-optical modulators.

CRediT authorship contribution statement

Andrea Schirato: Conceptualization, Methodology, Writing – original draft. **Margherita Maiuri:** Conceptualization, Investigation, Supervision, Writing – review & editing.

Declaration of competing interest

The authors declare that they have no known competing financial interests or personal relationships that could have appeared to influence the work reported in this paper.

Acknowledgements

This publication is part of the METAFAST project that received funding from the European Union Horizon 2020 Research and Innovation programme under Grant Agreement No. 899673. This work reflects only author view and the European Commission is not responsible for any use that may be made of the information it contains.

The authors thank Prof. Giuseppe Della Valle for the constructive discussions.

References

[1] M.L. Brongersma, Engineering optical nanoantennas, Nat. Photonics 2 (2008) 270–272, https://doi.org/10.1038/nphoton.2008.60.
[2] A.I. Kuznetsov, A.E. Miroshnichenko, M.L. Brongersma, Y.S. Kivshar, B. Luk'yanchuk, Optically resonant dielectric nanostructures, Science 354 (2016), https://doi.org/10.1126/science.aag2472, 6314 aag2472.
[3] N. Yu, F. Capasso, Flat optics with designer metasurfaces, Nat. Mater. 13 (2014) 139–150, https://doi.org/10.1038/nmat3839.
[4] A.V. Kildishev, A. Boltasseva, V.M. Shalaev, Planar photonics with metasurfaces, Science 339 (2013) 1232009, https://doi.org/10.1126/science.1232009.
[5] S.V. Makarov, A.S. Zalogina, M. Tajik, D.A. Zuev, M.V. Rybin, A.A. Kuchmizhak, S. Juodkazis, Y. Kivshar, Light-induced tuning and reconfiguration of nanophotonic structures, Laser Photon. Rev. 11 (2017) 1700108, https://doi.org/10.1002/lpor.201700108.
[6] M. Ren, W. Cai, J. Xu, Tailorable dynamics in nonlinear optical metasurfaces, Adv. Mater. 32 (2020) 1806317, https://doi.org/10.1002/adma.201806317.
[7] D. Neshev, I. Aharonovich, Optical metasurfaces: new generation building blocks for multi-functional optics, Light Sci. Appl. 7 (2018) 58, https://doi.org/10.1038/s41377-018-0058-1.
[8] F. Aieta, P. Genevet, M.A. Kats, N. Yu, R. Blanchard, Z. Gaburro, F. Capasso, Aberration-free ultrathin flat lenses and axicons at telecom wavelengths based on plasmonic metasurfaces, Nano Lett. 12 (2012) 4932–4936, https://doi.org/10.1021/nl302516v.
[9] H.-T. Chen, A. Taylor, N. Yu, A review of metasurfaces: physics and applications, Rep. Prog. Phys. 79 (2016), 076401, https://doi.org/10.1088/0034-4885/79/7/076401.
[10] M.R. Shcherbakov, P.P. Vabishchevich, A.S. Shorokhov, K.E. Chong, D.-Y. Choi, I. Staude, A.E. Miroshnichenko, D.N. Neshev, A.A. Fedyanin, Y.S. Kivshar, Ultrafast all-optical switching with magnetic resonances in nonlinear dielectric nanostructures, Nano Lett. 15 (2015) 6985–6990, https://doi.org/10.1021/acs.nanolett.5b02989.
[11] G. Della Valle, B. Hopkins, L. Ganzer, T. Stoll, M. Rahmani, S. Longhi, Y.S. Kivshar, C. De Angelis, D.N. Neshev, G. Cerullo, Nonlinear anisotropic dielectric metasurfaces for ultrafast nanophotonics, ACS Photonics 4 (2017) 9, https://doi.org/10.1021/acsphotonics.7b00544.

[12] P. Vasa, C. Ropers, R. Pomraenke, C. Lienau, Ultra-fast nano-optics, Laser Photon. Rev. 3 (2009) 483–507, https://doi.org/10.1002/lpor.200810064.
[13] G.A. Wurtz, R. Pollard, W. Hendren, G.P. Wiederrecht, D.J. Gosztola, V. A. Podolskiy, A.V. Zayats, Designed ultrafast optical nonlinearity in a plasmonic nanorod metamaterial enhanced by nonlocality, Nat. Nanotechnol. 6 (2011) 107–111, https://doi.org/10.1038/nnano.2010.278.
[14] M. Kauranen, A.V. Zayats, Nonlinear plasmonics, Nat. Photonics 6 (2012) 737, https://doi.org/10.1038/nphoton.2012.244.
[15] M. Brongersma, N.J. Halas, P. Nordlander, Plasmon-induced hot carrier science and technology, Nat. Nanotechnol. 10 (2015) 25–34, https://doi.org/10.1038/nnano.2014.311.
[16] A. Manjavacas, J.G. Liu, V. Kulkarni, P. Nordlander, Plasmon-induced hot carriers in metallic nanoparticles, ACS Nano 8 (2014) 7630–7638, https://doi.org/10.1021/nn502445f.
[17] L.V. Besteiro, P. Yu, Z. Wang, A.W. Holleitner, G.V. Hartland, G.P. Wiederrecht, A. O. Govorov, The fast and the furious: ultrafast hot electrons in plasmonic nanostructures. Size and structure matter, Nano Today 27 (2019) 120, https://doi.org/10.1016/j.nantod.2019.05.006.
[18] L.H. Nicholls, F.J. Rodríguez-Fortuño, M.E. Nasir, R.M. Córdova-Castro, N. Olivier, G.A. Wurtz, A.V. Zayats, Ultrafast synthesis and switching of light polarization in nonlinear anisotropic metamaterials, Nat. Photonics 11 (2017) 628–633, https://doi.org/10.1038/s41566-017-0002-6.
[19] M. Taghinejad, H. Taghinejad, Z. Xu, K.-T. Lee, S.P. Rodrigues, J. Yan, A. Adibi, T. Lian, W. Cai, Ultrafast control of phase and polarization of light expedited by hot-electron transfer, Nano Lett. 18 (2018) 5544–5551, https://doi.org/10.1021/acs.nanolett.8b01946.
[20] K. Wang, M. Li, H.-H. Hsiao, F. Zhang, M. Siedel, A.-Y. Liu, J. Chen, E. Devaux, C. Genet, T. Ebbesen, High contrast, femtosecond light polarization manipulation in epsilon-near-zero material coupled to a plasmonic nanoatenna array, ACS Photonics 8 (2021) 2791–2799, https://doi.org/10.1021/acsphotonics.1c00971.
[21] Y. Yang, K. Kelley, E. Sachet, S. Campione, T.S. Luk, J.-P. Maria, M.B. Sinclair, I. Brener, Femtosecond optical polarization switching using a cadmium oxide-based perfect absorber, Nat. Photonics 11 (2017) 390–395, https://doi.org/10.1038/nphoton.2017.64.
[22] Y. Wu, L. Kang, H. Bao, D.H. Werner, Exploiting topological properties of Mie-resonance-based hybrid metasurfaces for ultrafast switching of light polarization, ACS Photonics 7 (2020) 2362–2373, https://doi.org/10.1021/acsphotonics.0c00858.
[23] S. Klimmer, O. Ghaebi, A. George, A. Turchanin, G. Cerullo, G. Soavi, All-optical polarization and amplitude modulation of second-harmonic generation in atomically thin semiconductor, Nat. Photonics (2021), https://doi.org/10.1038/s41566-021-00859-y.
[24] A. Schirato, M. Maiuri, A. Toma, S. Fugattini, R. Proietti Zaccaria, P. Laporta, P. Nordlander, G. Cerullo, A. Alabastri, G. Della Valle, Transient optical symmetry breaking for ultrafast broadband dichroism in plasmonic metasurfaces, Nat. Photonics 14 (2020) 12, https://doi.org/10.1038/s41566-020-00702-w.
[25] A. Sugita, H. Yogo, K. Mochizuki, S. Hamada, H. Matsui, A. Ono, W. Inami, Y. Kawata, M. Yoshizawa, Polarization-resolved femtosecond pump-probe spectroscopy for Au nanodisks at the LSP resonance, OSA Continuum 3 (2020) 2943–2952, https://doi.org/10.1364/OSAC.406145.
[26] H. Baida, D. Mongin, D. Christofilos, G. Bachelier, A. Crut, P. Maioli P, N. Del Fatti, F. Vallée, Ultrafast nonlinear optical response of a single gold nanorod near its surface plasmon resonance, Phys. Rev. Lett. 107 (2011), https://doi.org/10.1103/PhysRevLett.107.057402, 5 057402.
[27] N. Del Fatti, F. Vallée, C. Flytzanis, Y. Hamanaka, A. Nakamura, Electron dynamics and surface plasmon resonance nonlinearities in metal nanoparticles, Chem. Phys. 251 (2000) 215–226, https://doi.org/10.1016/S0301-0104(99)00304-3.
[28] A. Brown, R. Sundararaman, P. Narang, A.M. Schwartzberg, W.A. Goddard III, H. A. Atwater, Experimental and ab initio ultrafast carrier dynamics in plasmonic nanoparticles, Phys. Rev. Lett. 118 (2017), 087401, https://doi.org/10.1103/PhysRevLett.118.087401.
[29] L.H. Nicholls, T. Stefaniuk, M.E. Nasir, F.J. Rodríguez-Fortuño, G.A. Wurtz, A. V. Zayats, Designer photonic dynamics by using non-uniform electron temperature distribution for on-demand all-optical switching times, Nat. comm. 10 (2019) 2967, https://doi.org/10.1038/s41467-019-10840-7.
[30] M. Conforti, G. Della Valle, Derivation of third-order nonlinear susceptibility of thin metal films as a delayed optical response, Phys. Rev. B 85 (24) (2012) 245423, https://doi.org/10.1103/PhysRevB.85.245423.
[31] C. Voisin, N. Del Fatti, D. Christofilos, F. Vallée, Ultrafast electron dynamics and optical nonlinearities in metal nanoparticles, J. Phys. Chem. B 105 (2001) 12, https://doi.org/10.1021/jp0038153.
[32] D. Polli, L. Lüer, G. Cerullo, G, High-time-resolution pump-probe system with broadband detection for the study of time-domain vibrational dynamics, Rev. Sci. Instrum. 78 (2007) 103108, https://doi.org/10.1063/1.2800778.
[33] J.G. Liu, H. Zhang, S. Link, P. Nordlander, Relaxation of plasmon-induced hot carriers, ACS Photonics 5 (2018) 2584–2595, https://doi.org/10.1021/acsphotonics.7b00881.
[34] S. Dal Conte, M. Conforti, D. Petti, E. Albisetti, S. Longhi, R. Bertacco, C. De Angelis, G. Cerullo, G. Della Valle, Disentangling electrons and lattice nonlinear optical response in metal-dielectric Bragg filters, Phys. Rev. B 89 (2014) 125122, https://doi.org/10.1103/PhysRevB.89.125122.
[35] C.-K. Sun, F. Vallée, L.H. Acioli, E.P. Ippen, J.G. Fujimoto, Femtosecond-tunable measurement of electron thermalization in gold, Phys. Rev. B 50 (1994) 15337, https://doi.org/10.1103/PhysRevB.50.15337.
[36] M. Zavelani-Rossi, D. Polli, S. Kochtcheev, A.-L. Baudrion, J. Béal, V. Kumar, E. Molotokaite, M. Marangoni, S. Longhi, G. Cerullo, P.M. Adam, G. Della Valle, Transient optical response of a single gold nanoantenna: the role of plasmon detuning, ACS Photonics 2 (2015) 521–529, https://doi.org/10.1021/ph5004175.
[37] A. Block, M. Liebel, R. Yu, M. Specto, Y. Sivan, F.J. García de Abajo, N.F. van Hulst, Tracking ultrafast hot-electron diffusion in space and time by ultrafast thermomodulation microscopy, Science Adv 5 (5) (2019), eaav8965, https://doi.org/10.1126/sciadv.aav8965.
[38] A. Rudenko, K. Ladutenko, S. Makarov, T.E. Itina, Photogenerated free carrier-induced symmetry breaking in spherical silicon nanoparticle, Adv. Opt. Mat. 6 (7) (2018) 1701153, https://doi.org/10.1002/adom.201701153.
[39] Y. Sivan, M. Spector, Ultrafast dynamics of optically induced heat gratings in metals, ACS Photonics 7 (2020) 5 1271–9, https://doi.org/10.1021/acsphotonics.0c00224.
[40] E. Carpene, Ultrafast laser irradiation of metals: beyond the two-temperature model, Phys. Rev. B 74 (2006), 024304, https://doi.org/10.1103/PhysRevB.74.024301.
[41] W.S. Fann, R. Storz, H.W.K. Tom, J. Bokor, Electron thermalization in gold, Phys. Rev. B 46 (1992) 13592, https://doi.org/10.1103/PhysRevB.46.13592.
[42] T. Labouret, B. Palpant, Nonthermal model for ultrafast laser-induced plasma generation around a plasmonic nanorod, Phys. Rev. B 94 (2016) 245426, https://doi.org/10.1103/PhysRevB.94.245426.
[43] L.V. Besteiro, X.-T. Kong, Z. Wang, G. Hartland, A.O. Govorov, Understanding hot-electron generation and plasmon relaxation in metal nanocrystals: quantum and classical mechanisms, ACS Photonics 4 (2018) 2759, https://doi.org/10.1021/acsphotonics.7b00751.
[44] A.P. Kanavin, I.V. Smetanin, V.A. Isakov, Y.V. Afanasiev, B.N. Chichkov, B. Wellegehausen, S. Nolte, C. Momma, A. Tünnermann, Heat transport in metals irradiated by ultrashort laser pulses, Phys. Rev. B 57 (1998) 14698, https://doi.org/10.1103/PhysRevB.57.14698.
[45] R. Rosei, F. Antonangeli, U.M. Grassano, d bands position and width in gold from very low temperature thermomodulation measurements, Surf. Sci. 37 (1973) 689–699, https://doi.org/10.1016/0039-6028(73)90359-2.
[46] J.H. Hodak, A. Henglein, G.V. Hartland, Size dependent properties of Au particles: coherent excitation and dephasing of acoustic vibrational modes, J. Chem. Phys. 111 (1999) 8613–8621, https://doi.org/10.1063/1.480202.
[47] O.L. Muskens, N. Del Fatti, F. Vallée, Femtosecond response of a single metal nanoparticle, Nano Lett. 6 (2006) 552–556, https://doi.org/10.1021/nl0524086.
[48] T.S. Ahmadi, S.L. Logunov, M.A. El-Sayed, Picosecond dynamics of colloidal gold nanoparticles, J. Phys. Chem. 100 (1996) 8053–8056, https://doi.org/10.1021/jp960484e.